Subproject B1.6

Single-Atom Transistors and Atomic-Scale Quantum Point Contacts by Electrochemical Deposition

Principle Investigators: Thomas Schimmel[1, 2]

CFN-Financed Scientists: F.-Q. Xie (1 BAT IIa, 60 months), Ch. Obermair (1 BAT IIa, 18 months) and (1/2 BAT IIa, 12 months), S. Zhong (3/4 BAT IIa, 3 months), P. Vincze (1/2 BAT IIa, 4 months), A. Peukert (1/4 BAT IIa, 4 months)

[1]Institute of Applied Physics and Center for Functional Nanostructures (CFN), Karlsruhe Institute of Technology (KIT), Campus South, 76131 Karlsruhe, Germany

[2]Institute of Nanotechnology and Center for Functional Nanostructures (CFN), Karlsruhe Institute of Technology (KIT), Campus North, 76021 Karlsruhe, Germany

Single-Atom Transistors and Atomic-Scale Quantum Point Contacts by Electrochemical Deposition

Introduction and Summary

Due to their interesting physical properties and potential technological perspectives, metallic quantum wires and atomic-scale contacts are an object of intensive experimental and theoretical investigations [1]. As the size of these constrictions is smaller than the scattering length of the conduction electrons, transport through such contacts is ballistic, and as the width of the contacts is on the length scale of the electron wavelength, the quantum nature of the electrons is directly observable. Different experimental techniques have been developed for the fabrication of atomic-scale point contacts, namely mechanically controlled break junctions (MCBJ) [2], modified scanning tunneling microscopes (STM) [3], electromigration [4], and electrochemical methods [5]. Whereas in break junction experiments and STM-based setups, atomic-scale contacts are formed by plastic deformation of the contact area, the advantage of the electrochemical deposition method is the absence of mechanical strain during contact formation. Subproject B1.6 is concerned with the electron transport, bi-/multistabilities in metallic atomic-scale point contacts fabricated with the electrochemical method, and the exploration of their bi-/multistabilities for atomic-scale conductance switches. The devices, which reproducibly operate at room temperature, open fascinating perspectives towards quantum electronics and logics on the atomic scale.

- **Preselectable integer quantum conductance of electrochemically fabricated silver point contacts**

The controlled fabrication of well-ordered atomic-scale metallic contacts is of great interest: it is expected that the experimentally observed high percentage of point contacts with a conductance at non-integer multiples of the conductance quantum $G_0=2e^2/h$ in simple metals is correlated to defects resulting from the fabrication process. Here we demonstrate a combined electrochemical deposition and annealing method which allows the controlled fabrication of point contacts with preselectable integer quantum conductance. The resulting conductance measurements on silver point contacts are compared with tight-binding-like conductance calculations of modeled idealized junction geometries between two silver crystals with a predefined number of contact atoms.

- **Independently switchable atomic quantum transistors by reversible contact reconstruction**

The controlled fabrication of actively switchable atomic-scale devices, in particular transistors, has remained elusive to date. Here, we explain the operation of an atomic-scale three-terminal device by a novel switching mechanism of bistable, self-stabilizing reconstruction of the electrode contacts at the atomic level: While the device is manufactured by electrochemical deposition, it operates entirely on the basis of mechanical effects of the solid-liquid interface. We analyze mechanically and thermally stable metallic junctions with a predefined quantized conductance of 1–5 G_0 in experiment and atomistic simulation. Atomistic modeling of structural and conductance properties elucidates bistable electrode reconstruction as the underlying mechanism of the device.

- **Integrated circuit of atomic-scale transistors**

A prototype integrated circuit of atomic-scale transistors has been demonstrated with the electrochemical fabrication approach. Such devices may be manufactured using conventional,

abundant, inexpensive, and nontoxic materials and possess extremely nonlinear current-voltage characteristics, desirable in many applications. Their electrode arrays can be deposited with lithography, making devices compatible with existing electronics. Because the switching process is achieved with very small gate potential (mV), the power consumption of such devices may be orders of magnitude lower than that of conventional semiconductor-based electronics. Integrated circuits based on this novel principle of operation represent a completely new class of quantum electronic devices.

- **Multilevel atomic-scale transistors based on metallic quantum point contacts**

We have demonstrated multilevel metallic quantum point contact transistors. These devices can be switched reversibly between different quantized (non-zero) conductance levels by fabrication of bi- and multistable configurations on the atomic scale. The devices reproducibly operate at room temperature, the source-drain conductance being switched by a control voltage applied to an independent third gate electrode. Computer simulations allow a detailed understanding of the multilevel switching process based on bi- and multistable atomic-scale reconstruction of the contact configuration. The results allow to configure model systems for studying conductance quantization and atomic-scale reconfigurations in predefined, switchable systems. At the same time they open intriguing perspectives for multilevel logics and quantum electronics at the atomic scale.

- **Atomic-scale nonvolatile transistors fabricated within a gel electrolyte**

A gel electrolyte was made by mixing colloidal silicon dioxide with an aqueous solution of silver nitrate and nitric acid. The electrochemical properties of the gel electrolyte were characterized by cyclic voltammetry. For comparision, cyclic voltammograms of the aqueous and gel electrolyte were measured under the same conditions and showed only small deviations. The operation of an atomic-scale non-volatile transistor has been demonstrated in such kind of gel electrolyte. Progress on solidification of the device has been made with the gel electrolyte. It represents an atomic relay, quantum switch, and non-volatile memory, opening intriguing perspectives for the emerging fields of quantum electronics, logics, and memory on the atomic scale.

- **Conductance of atomic-scale Pb contacts and their conductance switching in an electrochemical environment**

The high thermal and mechanical stability and low strain in our electrochemically fabricated atomic Pb contacts made it possible to resolve sharp conductance peaks and detailed substructures within the broad first peak in the conductance histograms previously obtained with MCBJ or STM techniques. The theoretical analysis of transport within an DFT approach yields junction geometries explaining the peaks at 1.4 G_0 and 2.8 G_0 and allows to attribute them to neutral single-atom and dimer Pb contacts. The results demonstrate that – depending on the local contact geometry of the surrounding atoms – single-atom contacts of one and the same metal can have different quantized conductance values.

In the timeframe 2006–2010, Subproject B1.6 (including its predecessor project B2.3) has led to 11 publications, among which are 1 article in *Nano Lett.*, 1 in *Adv. Mater.,* 1 in *Appl. Phys. Lett.*, 1 in *Phys. Rev.B,* 1 in *Europhysics News.,* 1 in *Small.* Approx. 30 invited and plenary talks were given in international meetings.

1. Preselectable integer quantum conductance of electrochemically fabricated silver point contacts [B1.6:2]

To produce well-ordered contacts, a technique of nearly defect-free growth by slow quasi-equilibrium deposition is required, which can be provided by electrochemical deposition methods. In addition, techniques of electrochemical annealing provide the possibility of healing atomic-scale defects in contacts even after fabrication (see below). Due to its high electrochemical exchange current density, silver is a promising candidate for efficiently applying electrochemical annealing techniques.

In this section we demonstrate an electrochemical annealing method by electrochemical deposition/dissolution cycling of atomic-scale silver contacts and compare the experimentally observed conductance with the calculated conductance of modeled idealized junctions between two ideal single crystals with a predefined number of contacting atoms.

The experimental set-up is shown in Fig. 1(a). By applying an electrochemical potential, silver was deposited within the gap between two macroscopic gold electrodes. Two silver wires served as counter and quasi-reference electrodes. The potentials of the working electrodes with respect to the quasi-reference and counter electrodes were set by a computer-controlled bipotentiostat. During deposition, the conductance between the two gold electrodes was continuously measured. As soon as a predefined conductance value was exceeded, the computer-controlled feedback immediately stopped further deposition of silver on the working electrodes. If desired, the deposited contact could be fully or partially electrochemically dissolved by applying an electrochemical potential.
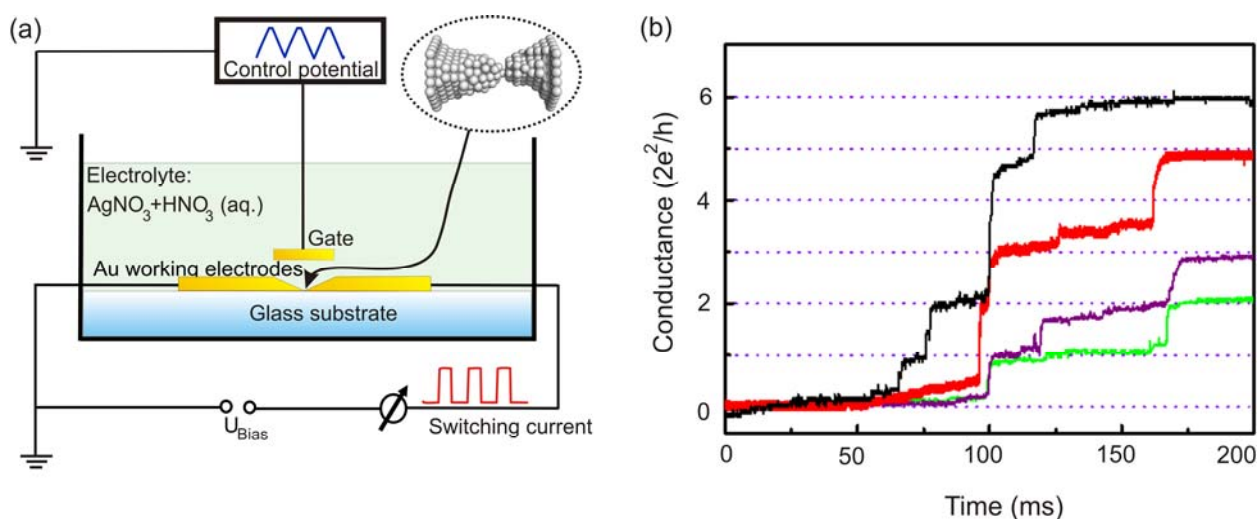

Fig. 1. (a) Schematic diagram of the experimental setup. (b) "Atomic Fingerprinting": Detection of atomic-level reconfigurations and transient levels via conductance-vs.-time measurements. The diagram shows the conductance of four different silver point contacts during contact formation within initial electrochemical deposition, all four finally ending at a stable level at an integer multiple of the conductance quantum $G_0 = 2e^2/h$.

Figure 1(b) shows conductance-vs.-time curves of the closing processes of four different atomic-scale contacts during initial deposition, i.e. before electrochemical annealing. In this way, initially, contacts of limited stability were formed, typically exhibiting conductance values which are *non-integer* multiples of G_0. Now, a dissolution/deposition cycle between predefined conductance values was performed: after the initial deposition cycle, a dissolution potential was applied until the

conductance dropped below a predefined lower threshold. Subsequently, deposition was started once more until conductance exceeded a predefined upper threshold. At this point, a new dissolution/deposition cycle was started and so on. Typically, after a number of cycles, a stable contact was formed, which exhibited an integer conductance value, and the cycling was stopped. Using this method, stable conductance levels at integer multiples of G_0 were configured. Examples for $n \cdot G_0$ ($n = 1, 2, 3, 4, 5$) are given in Fig. 2(a). This transition from instable contacts with non-integer conductance to stable contacts with integer conductance values can be explained by an electrochemical annealing process, which heals defects in the direct contact region by electrochemical deposition and dissolution leading to an optimized contact configuration.

In order to get insights into the possible structures of the measured point contacts, we calculated the coherent conductance of ideal crystalline silver nanojunctions (see Fig. 2(b)). Geometries were generated by assuming two fcc electrode clusters, which are connected at their tips by a small number of Ag-Ag-bridges in [111] direction with a bond length of 2.88 Å. As shown in Fig. 2(b), nearly integer conductance of the idealized geometries was found for contact geometries #1 … #5: $0.97\ G_0$, $1.95\ G_0$, $2.89\ G_0$, $3.95\ G_0$, $4.91\ G_0$, respectively. The deviation from integer multiples of G_0 of about $0.1\ G_0$ is within the range of the accuracy of the numerical method. A good correlation has been observed between the number of silver atoms at the point of minimal cross section and the number of conductance quanta, which aids in the construction of geometries with a particular value of the conductance.

In order to study to which extent the conductance values change due to geometrical changes in the interatomic distance of the contacting atoms and the relative angle between the contacting crystals, we introduced finite changes in contact geometry: we calculated the electrode distance and twist-angle dependence of the zero bias conductance. Increasing the electrode distance to twice the Ag-Ag bond length leads to a decrease by 86.7 % in the conductance, while twisting the electrodes by 60° against each other leads to a decrease of conductance of 22.0 %.
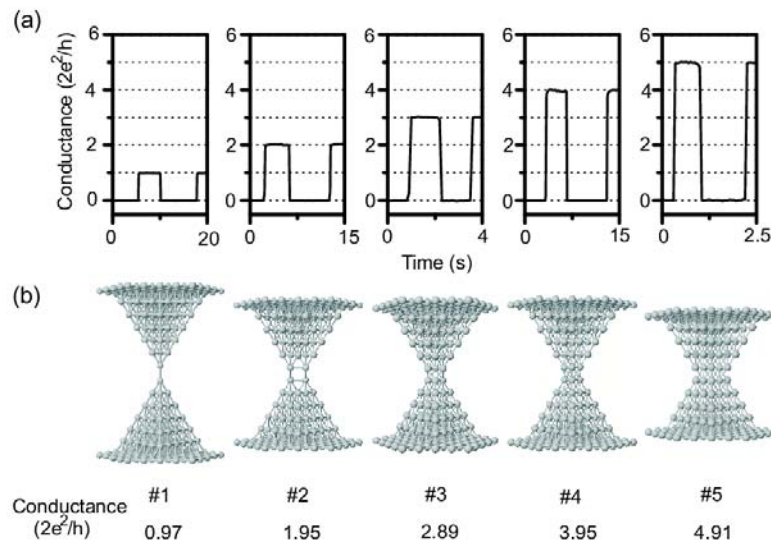

Fig. 2. Comparison of experimental conductance data of electrochemically annealed silver point contacts with calculations assuming idealized geometries. (a) Quantum conductance of five different annealed atomic-scale contacts. (b) Idealized geometries of silver point contacts with predefined numbers of contacting atoms.

2. Independently switchable atomic quantum transistors by reversible contact reconstruction [B1.6:1]

We have developed a three-terminal gate-controlled atomic quantum switch with a silver quantum point contact in an electrochemical cell, working as an atomic-scale relay [8]. We control individual atoms in a quantum point contact by an independent gate electrode, which allows a reproducible switching of the contact between a quantized conducting "on-state" and an insulating "off-state" (Fig. 3(a)).

When we set the gate potential to an intermediate "hold" level between the "on" and the "off" potentials, the currently existing state of the atomic switch remains stable, and no further switching takes place. This is demonstrated in Fig. 3(b) both for the "on-state" of the switch (left arrow) and for the "off-state" of the switch (right arrow). Thus, the switch can be reproducibly operated by the use of three values of the gate potential for "switching on", "switching off", and "hold". This provides the basis for atomic-scale logical gates and atomic-scale digital electronics.

The smallest observed conductance value was $1\,G_0$, but we have significantly optimized our protocol to configure quantum conductance switches with any integer multiple $1 \leq n \leq 5$ of G_0 at will (see Fig. 4 (left)). Fig. 4 (middle) shows representative conformations of simulated junctions, computed zero-bias conduction, and number of junctions with the specified conductance. Representative minimal cross-sections for each conductance level is plotted in Fig. 4 (right). The minimal cross-sections are characteristic for each group of the switch conformers and determine their quantized conductance

While we can understand the conductance properties of such junctions on the basis of atomistic conductance calculations, the physical process underlying the switching mechanism remained unclear. Reproducible switching between quantum conductance levels over many cycles cannot be explained by conventional atom-by-atom deposition but requires a collective switching mechanism. Theoretical previous calculations have shown that only well-ordered junction geometries result in integer multiples of the conductance quantum [B1.6:2]. Neither partial dissolution of the junction nor its controlled rupture yields the necessary atomic-scale memory effect. A more detailed model of the structural and conductance properties of such junctions is therefore required.
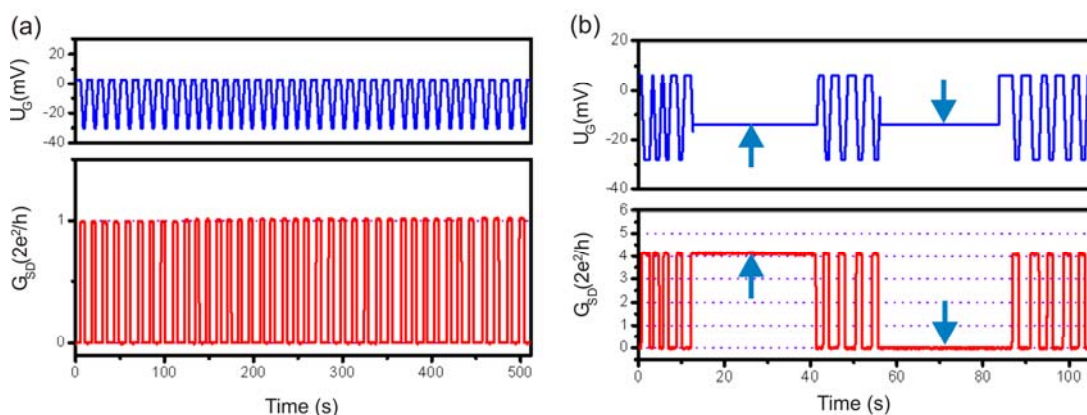

Fig. 3. Switching current by electrochemical, gate-controlled atomic movement. (a) Realization of switching current reproducibly with a single-atom point contact between 0 and $1\,G_0$. (b) Demonstration of quantum conductance switching between 0 and $4\,G_0$.
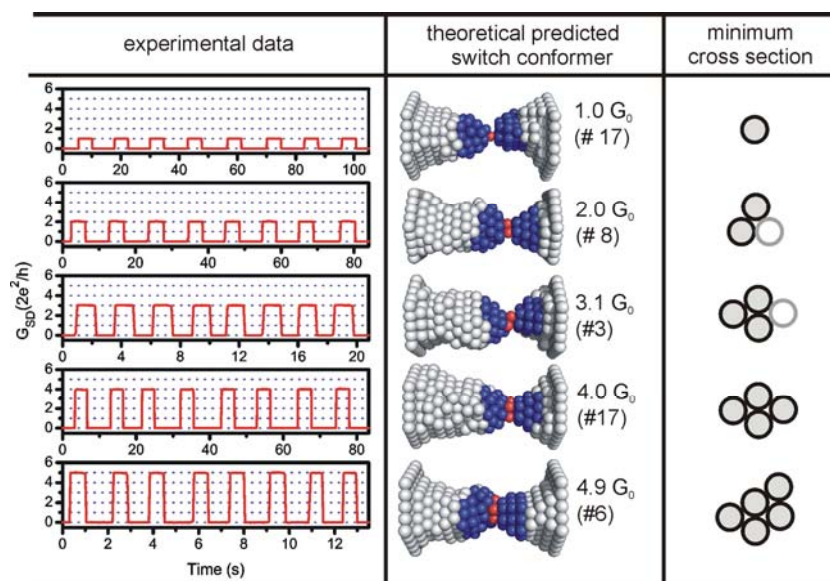
Fig. 4. Relation between the structures of atomic point contacts and their conductance.

The *switching mechanism* was investigated in close cooperation with theoretical groups within the CFN (see below, chapter 6). The theoretical simulation data rationalize the bistable reconfiguration of the electrode tips as the underlying mechanism of the formation of nanojunctions with predefined levels of quantum conductance. These levels are determined by the available bistable junction conformations, similar to magic numbers for metal clusters, that are most likely material-specific. For silver, the observed quantum conductance levels appear to coincide with integer multiples of the conductance quantum. When we form a junction by halting the deposition process at a noninteger multiple of G_0 (both experimentally and in simulation), subsequent switching cycles either converge to an integer conductance at a nearby level or destroy the junction. By snapping into "magic" bistable conformations, junctions are mechanically and thermally stable at room temperature for long sequences of switching cycles. This process is assisted by the electrochemical environment but not intrinsically electrochemical: The reproducible switching of large junctions by coordinated dissolution/regrowth of the junction is very unlikely.
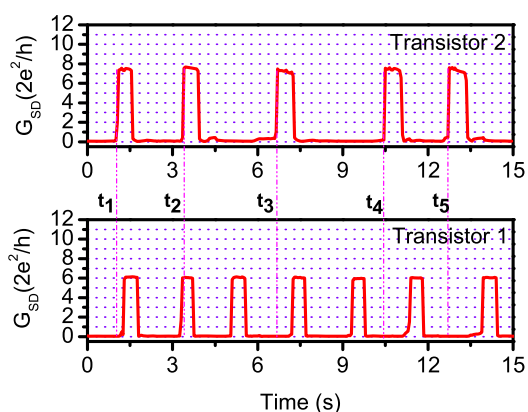

Fig. 5. Parallel and independent operation of two atomic transistors grown on one and the same substrate chip in a common electrolyte.

The electrochemical fabrication approach permits parallel device deposition between multielectrode arrays structured by lithography. We have varied the deposition protocol to subsequently deposit two atomic transistors on one and the same substrate chip. In Fig. 5, we demonstrate that these transistors can be operated independently and in parallel in a common electrolyte. Each of the transistors is controlled by its own individually addressable switching potential. This operation of

two transistors independently on the same chip constitutes the simplest form of an integrated circuit operating on the atomic scale.

3. Multilevel atomic-scale transistors based on metallic quantum point contacts [B1.6:11]

Recently, we demonstrated a multilevel atomic quantum transistor, allowing for the gate-controlled switching between *different* quantized conducting states. Multilevel logics and storage devices on the atomic scale are of great interest as they allow for a more efficient data storage and processing with a smaller number of logical gates. The experiments are combined with detailed computer simulations, allowing a profound understanding of the multilevel switching process. The results provide a basis for the future development of ultra-small devices for multilevel logics on the atomic scale.

Our experiments show that such a controlled switching between *two* conducting "on-states" can be implemented by manipulating the atomic configuration within the junction applying an electrochemical cycling technique.

Figure 6 gives a first demonstration of the operation of an atomic transistor switching not between zero and a conductance level G_1, but between *two different* quantized non-zero conductance levels G_1 and G_2. The upper diagram of Fig. 6(a) gives the control potential (blue) as a function of time, while the lower diagram shows the resulting, simultaneously recorded conductance-vs.-time curve (red), respectively. The two states exhibit conductance levels of $G_1 = 3.0\,G_0$ and $G_2 = 5.0\,G_0$, respectively. Sharp transitions are observed between the two conductance levels. Fig. 6(b) gives a further example of an interlevel quantum transistor, in this case switching between the conductance levels of $G_1 = 1.0\,G_0$ and $G_2 = 3.0\,G_0$, respectively. The observed reproducible switching can be explained by the formation of two highly stable atomic configurations of the contact area corresponding to two different quantized "on-state" conductance values, between which the contact is transformed or "switched" reversibly by applying the corresponding control potential. Fig. 6(c) gives an example for a transition from a switching sequence between zero and *one* finite conductance value to the switching sequence between *two* different finite values. Three distinct, stable configurations of the contact are identified at zero conductance, a lower quantized conductance level at $1.0\,G_0$ and a higher quantized conductance level at $3.0\,G_0$ from the experimental data. In both cases the upper levels are the same. Before the time indicated by the arrow, the conductance is switched reversibly between 0 and $3\,G_0$. After the time indicated by the arrow in Fig. 6(c) the contact does not open completely any more but the conductance remains at a level of $1\,G_0$ in the lower conductance level, subsequently switching reproducibly between the two conducting states of $1\,G_0$ and $3\,G_0$. This observation excludes a switching mechanism by superposition of two independent, parallel point contacts. It rather indicates true multilevel switching between different configurations of *one and the same* point contact.

In close cooperation with the theory group of W. Wenzel (subproject C3.6), the corresponding calculations were performed. In order to explain the multilevel conductance switching in the experimental data described above, atomic structure computer simulations of opening/closing processes in silver nanojunctions were combined with zero bias conductance calculations. The theoretical results are in good agreement with our experimental observations and confirm the above described model of a bistable structural switching of the contacting cluster of atoms [B1.6:11].
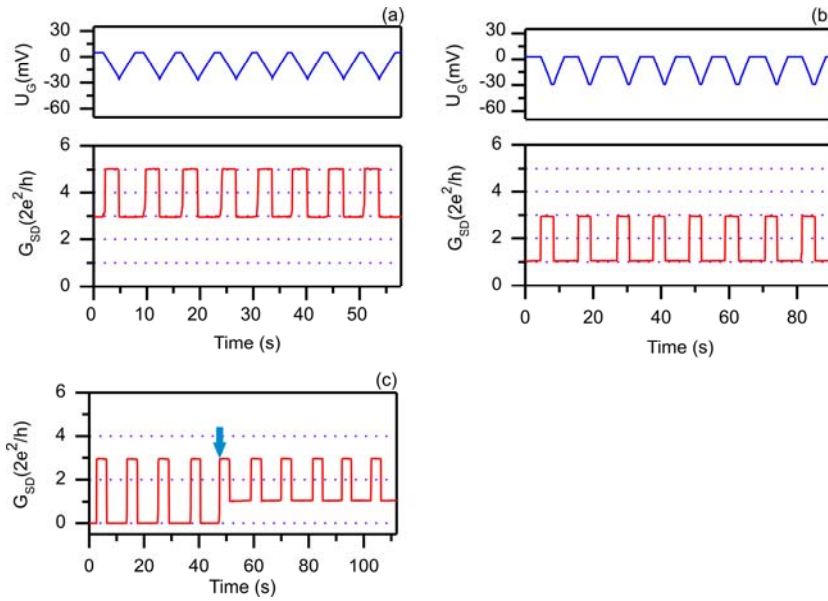
Fig. 6 (a) and (b): Experimental demonstration of the operation of interlevel transistors based on an atomic-scale point contact. (c) Experimental demonstration of a multilevel atomic-scale transistor switching between an "off-state" and two different "on-states".

4. Atomic-scale nonvolatile transistors fabricated within a gel electrolyte

The replacement of the fluid aqeous electrolyte with a solid electrolyte is one way to produce a nonvolatile transistor. However, solid electrolytes experience some stress after cycling of the deposition/dissolution procedure [7]. Silica gel is a random porous media with porous dimensions in the 10 nm range. It can contain a lot aqueous electrolyte in the porous space, and is soft after mixing with aqueous electrolyte. Here, we explored the electrochemical properties of the silica gel electrolyte and fabricated silver atomic-scale nonvolatile transistors within it.

Figure 8 (a) shows a photo of our sample covered with the gel electrolyte. The reference- and counter-electrodes are put into the gel electrolyte near the gap between two working electrodes. The electrochemical properties of the gel electrolyte were investigated by cyclic voltammetry. For comparison, the cyclic voltammetry experiments were performed both on the aqueous and gel electrolyte with the same conditions. The current density ($\mu A/mm^2$) is plotted against the quasi-reference potential U (V vs. Ag/Ag^+) as cyclic voltammograms in Fig. 8 (b). The maxima of the current density are found at -0.04 V, 0.06 V, 0.41 V and 0.51 V. In the range between -0.3 V and 0.3 V silver deposits on or dissolves from the working electrode. The maxima at -0.04 V and 0.06 V are related to the silver ion (Ag^+) reduction and silver atom oxidation, respectively. The potential windows for the silver deposition/dissolution, hydrogen and oxygen development are the same for both electrolytes. Only the amplitude of the current density shows some difference at the peak position. The potential parameters and the training process for the silver atomic-scale transistor in aqueous electrolyte could be utilized in this gel electrolyte.
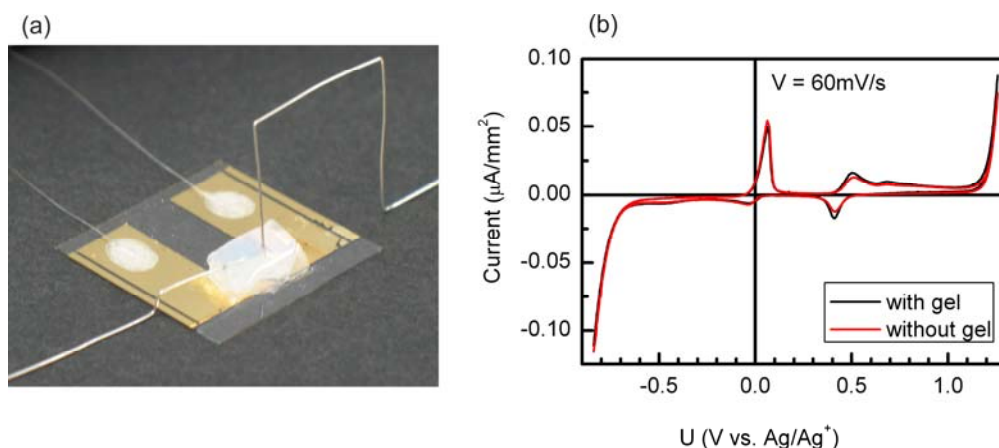
Fig. 8 (a) Photo of a sample covered with the gel electrolyte. (b) Comparison of cyclic voltammograms measured in an aqueous electrolyte (red) and a gel electrolyte (black).

The fabrication of silver atomic-scale point-contacts and training process for atomic switching in the gel electrolyte are similar as those in the aqueous electrolyte, which have been described in details in Reference 6. Fig. 9 (a) gives an example of a sequence of four controlled switching events, which are directly correlated to the electrochemical control potential applied to the gate electrode. The left upper diagram gives the control potential as a function of time, while the lower left diagram shows the simultaneously recorded resulting conductance-vs.-time curve. Each switching of the control potential is followed by a corresponding switching of the conductance level of the atomic-scale quantum switch. The switching processes do not occur immediately after the control potential is changed, but there is a characteristic delay time of several seconds between the change of the control potential and the resulting switching process. After each switching process, the control potential was set back by the computer to induce the opposite switching process, and after the mentioned characteristic delay time, the resulting switching process occurred. Delay times of this order are well-known in electrochemistry and represent typical time scales for the formation or change of the electrochemical diffusion layers as a result of a change of the applied electrochemical potential [8].

Apart from controlled switching between 0 and 2 G_0, it was also possible to configure quantum conductance switches which are capable of controlled switching between zero and a predefined integer multiple n of G_0. This was achieved by selecting a different value of the upper threshold conductance during the repeated cycling process. If, for example, a switch with a predefined on-state conductance of n G_0 should be fabricated, the upper threshold conductance during the repeated cycling process was set to a value of almost n G_0. As a result, during this cycling process, an atomic-scale switch was grown which reproducibly switched between zero and an on-state conductance of n G_0. In this way, the controlled fabrication of atomic-scale relays switching between zero and predefined higher quantized conductance levels was achieved. Stable and reproducible switching was observed, if these conductance levels, at which the upper threshold value for electrochemical cycling was set, were integer multiples of G_0. The upper and lower diagrams of Figs. 9(b) demonstrate bistable atomic-scale switching between 0 G_0 and 3 G_0 and between 0 G_0 and 4 G_0. In three cases, reproducible switching was achieved, the experimentally observed deviations of the on-state conductance from the ideal quantized values of 3 G_0 and 4 G_0, being only 0.7 % and 1.6 %, respectively. Theoretical calculations by Brandbyge et al. [9] predict that deviations of the conductance from integer multiples of G_0 will occur both due to point defects within the point contact or near its surface and due to surface roughness in the region of the point contact. The fact that the experimentally observed values are very close to integer multiples of G_0 indicates that the switching contacts are free of such defects even at higher multiples of G_0 and have

no strongly corrugated potential at their surface. The existence of silicic gel in the electrolyte has no obvious influence on the electron transport in the atomic-scale point-contacts. The stability of the atomic-scale switches and contacts in the presence of oxygen is remarkably high. Stable atomic-scale silver contacts were observed for several days and even more than one week in our experiments, although the experiments were performed at ambient conditions without exclusion of oxygen. One step toward the solidification of the metallic atomic-scale transistor has been made in this kind of gel electrolyte.
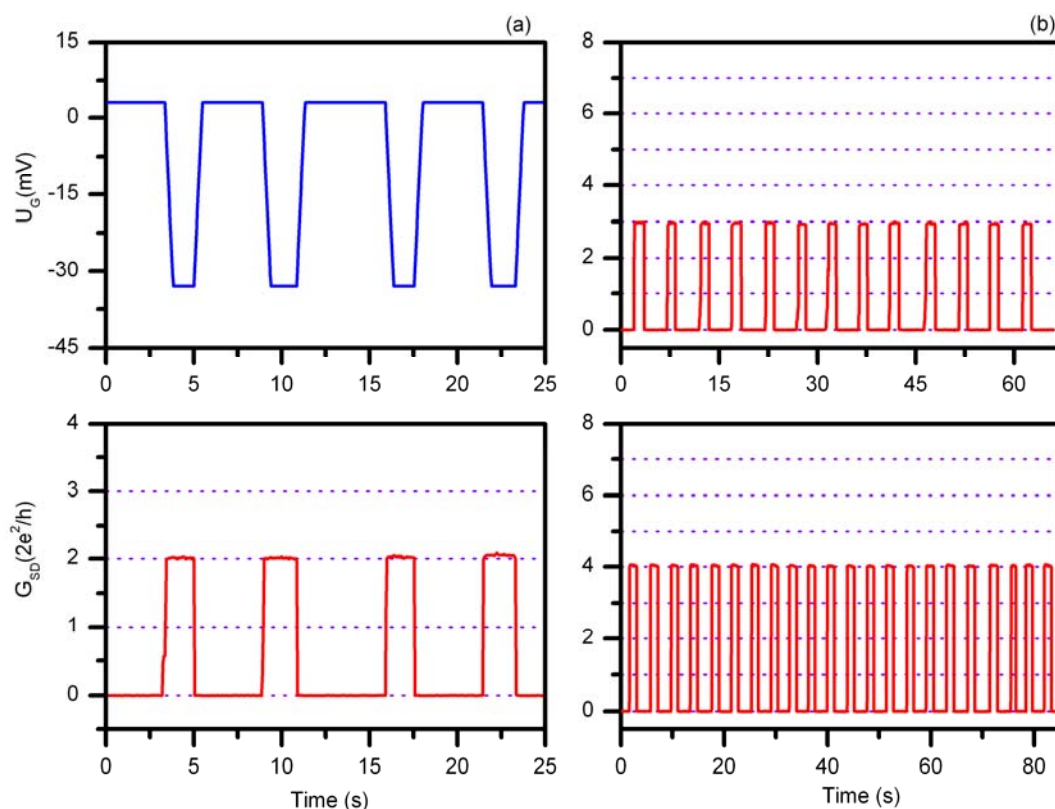

Fig. 9. Quantum conductance switch of an atomic-scale transistor in a gel electrolyte. Left, the control potential applied to the reference or "gate" electrode is illustrated in the upper diagram (a) in blue, while the corresponding conductance switching is plotted in the lower diagram in red (a). Two additional examples of controlled conductance switching within a gel electrolyte are shown in (b).

5. Conductance of atomic-scale Pb contacts and their switching in an electrochemical environment [B1.6:9]

Within this subproject, we also demonstrated experimentally first atomic quantum point contacts and atomic transistors on the basis of lead. The transport properties of atomic-scale contacts of Pb are of great interest, as Pb serves as a model system for multivalent metals. Our experiments were closely correlated with theoretical work within the CFN (F. Pauly, Subproject B1.7). So far, for Pb atomic contacts, only a broad peak between $1\,G_0$ to $3\,G_0$ was observed based on the MCBJ technique [10,11]. During stretching of the junctions, the plateau regions of the conductance traces commonly exhibit a negative slope as a result of the mechanical strain [11,12]. With electrochemical techniques we now have fabricated atomic-sized Pb contacts with a high thermal and mechanical stability, and exploited this for constructing gate-controlled atomic switches. We analyzed transport through atomic-sized Pb contacts both experimentally and theoretically. The

11

conductance histogram was compared to literature and theoretical results for ideal contact geometries. In DFT-based calculations we explored both single-atom and dimer geometries with a single atom or a "chain" of two atoms in the narrowest part of the junction, respectively. For these configurations, orientations of the semi-infinite electrodes along the three main crystallographic directions, namely [100], [110], and [111] were considered.

Our specially designed experimental setup is schematically illustrated in Fig.10(a). As lead oxidizes under ambient conditions, the electrochemical cell is shielded in an inert gas chamber. For the fabrication of Pb point contacts, two working electrodes made of gold and separated by a gap of approx. 50 nm are prepared. To minimize ionic conduction, they are covered with an insulating polymer coating except for the immediate contact area. Two lead wires are used for the quasi-reference and the counter electrodes. The potentials of the working electrodes with respect to the reference electrode and the counter electrode are set by a computer-controlled potentiostat. The electrolyte consists of 1 mM $Pb(NO_3)_2$ + 0.1 M HNO_3 in bi-distilled water. For conductance measurements, an additional voltage of -12.9 mV was applied between the two working electrodes. To exclude possible specific effects of the gold electrodes, contacts were also grown using Pb electrodes, yielding comparable results.

To fabricate the Pb contact within the gap between the two working electrodes, a potential of 10–20 mV was applied to the reference electrode. While lead was deposited in the junction, we monitored the conductance between the working electrodes. After contact deposition, the contact was opened again by setting the electrochemical potential of the reference electrode to a value between -18 mV and -36 mV, and closed again by choosing the potential between 6 mV and 15 mV. By continuously repeating this procedure, conductance-vs.-time traces were recorded for large numbers of opening and closing processes.
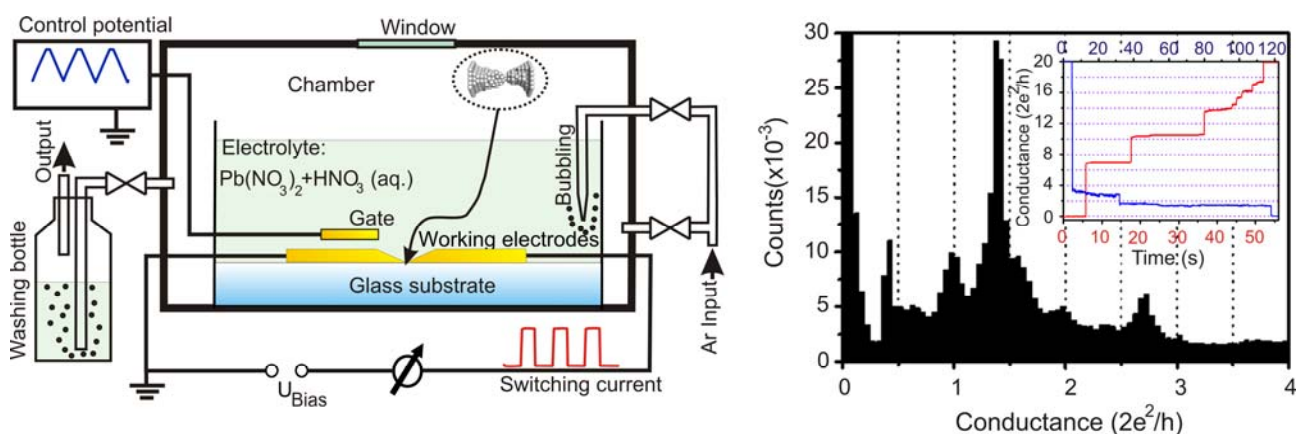

Fig. 10 (left) Specially designed experimental setup for Pb point contacts. (right) Conductance histogram of electrochemically fabricated atomic-scale Pb contacts. The inset shows two typical conductance traces for closing and opening processes.

Two typical conductance traces obtained for contact opening and closing are shown in the inset of Fig. 10 (right). The plateau regions in the traces typically are quite flat, a fact that can be explained by the lack of mechanical strain during the electrochemical growth process, in contrast to contacts fabricated with the MCJB or STM techniques, where mechanical deformations are involved. The trace shown in the inset of Fig. 10 (right) measured during dissolution exhibits two plateaus at around 2.8 G_0 and 1.4 G_0, the latter being consistent with results reported in Ref. [12, 14]. Furthermore, Fig. 10(b) shows a conductance histogram. It is plotted with a bin-size of

0.05 G_0 ($G_0 = 2e^2/h$) and represents the data from 1.5×10^6 conductance terraces in the conductance range between 0 and 20 G_0 for both deposition and dissolution from 64 different samples. The structure of the histogram with its most dominant peak at 1.4 G_0 differs clearly from those obtained with the MCBJ approach, where only a single, broad peak was observed between 1–3 G_0 and no detailed structure within this peak could be resolved. Here – most probably due to the lack of mechanical strain and structural defects within the junction area – a detailed substructure is resolved within this peak, demonstrating the advantages of the electrochemical deposition method. The peak position at 1.4 G_0 is consistent with results reported in Ref. [14]. Additional peaks in the conductance distribution are found at 1.0 G_0 , at 2.0 G_0 and at 2.8 G_0. In the range of 3–6 G_0, the conductance distribution in the histogram is quite flat and shows a low broad maximum centred at around 4.8 G_0. Corresponding to all maxima peaks in the conductance histogram, atomic-scale conductance switching was also realized with the Pb point contacts, which are illustrated below in Fig. 11(c).
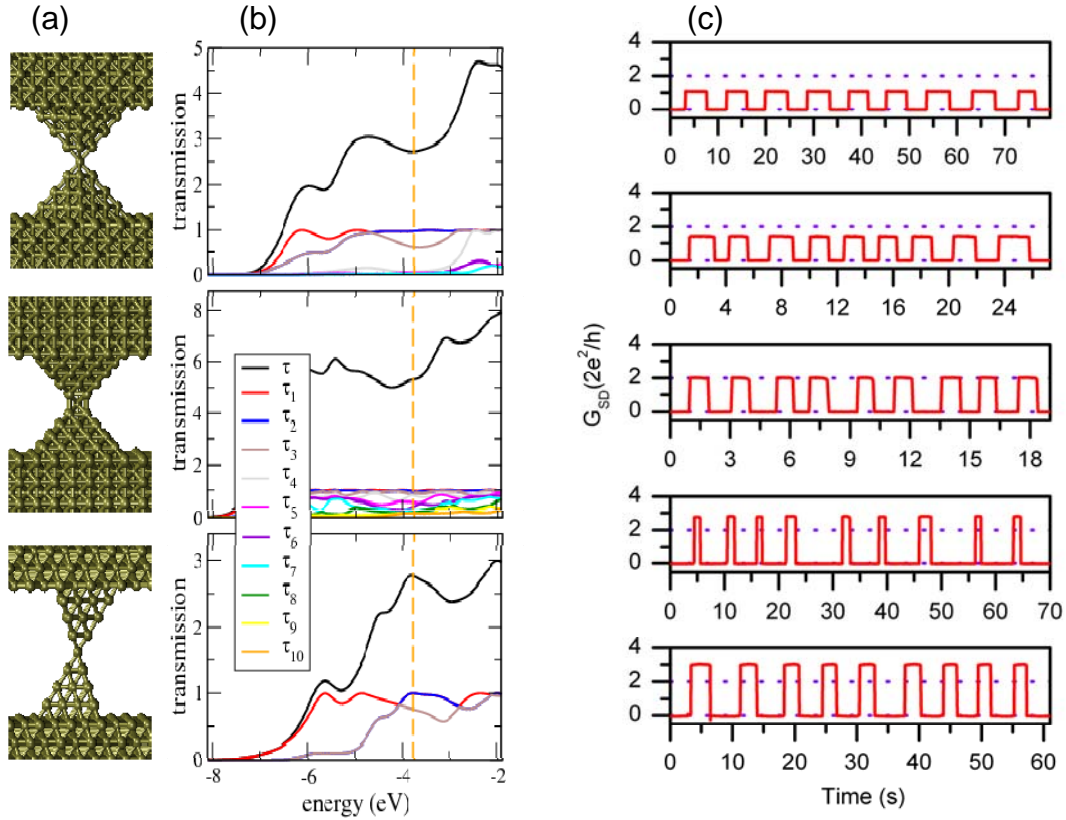

Fig. 11. Geometries of single-atom contacts (a), their transmission as a function of energy (b), and atomic-scale conductance switching realized with the Pb point contacts (c). The transmission τ is resolved into the contributions τ_i from individual conduction channels. The crystallographic orientation of the semi-infinite electrodes is [100] (upper), [110] (middle) and [111] (lower), respectively. The vertical yellow dashed lines indicate the Fermi energy at E_F = -3.76 eV.

Two types of junction configurations, namely single-atom and dimer contacts, were also investigated theoretically [B1.6:9]. For these contacts, different crystallographic orientations of the electrodes, namely [100], [110], and [111] were studied. Such geometries are believed to be responsible for the first peak in conductance histograms of metals under UHV conditions. Only ideal geometries were studied, where all atoms are located in the positions of the fcc lattice.

Calculated results for the single-atom contacts are displayed in Fig. 11(b). The transmission τ is resolved into the contributions τ_i from individual conduction channels. The crystallographic orientation of the semi-infinite electrodes is [100] (a, upper) [110] (a, middle) and [111] (a, lower), respectively. The yellow vertical dashed line in Fig. 11 (a) indicates the Fermi energy at $E_F = -3.76$ eV.

From the transmission at the Fermi energy, we obtain conductance G of 2.7 G_0, 5.3 G_0, and 2.8 G_0 for the [100], [110], and [111] directions, respectively. At first glance, the conductance for the [110] direction is surprisingly high. However, as visible in Fig. 11(a, middle) that contact should better be considered as "four-atom contact" due to the additional bonds resulting from the small distance of atomic layers. Therefore, that contact should be excluded from all further discussion, and will be referred to single-atom contacts as those for the [100] and [111] directions. For the latter two structures, the transmission at E_F is dominated by three transmission channels. From the LDOS of the atom in the narrowest part of the constriction, it is visible that the 6s and 6p states are responsible for conduction. Due to the high symmetry of the ideal contact structures, the transmission channels are degenerate for p_x and p_y for [100] and [111] orientations with symmetry D_{4h} and D_{3d}, respectively. Due to the lower D_{2h} symmetry of the [110] geometry, this degeneracy is lifted. This fact will be more clearly visible for the dimer junctions with their lower conductance (not shown here).

To conclude, the peaks at 1.4 G_0 and 2.8 G_0 in our histogram of Fig. 10 (right) are in good agreement with the corresponding theoretical results for single-atom and dimer structures, indicating that the contacts observed in the experiment are ideal lead contacts without contaminations, oxidation or structural defects, as each of these would lead to deviations from these conductance values.

The experimentally observed pronounced conductance peak at 1.0 G_0 is not predicted by the conductance calculations. However, as the contacts are in an aqueous electrochemical environment, small heteroatomic, molecular or ionic species working as bridges between the two atomic-scale lead electrodes such as traces of H_2, O, O_2, OH^- have to be taken into account. This is encouraged by the fact that in previous break junction experiments, the value of 1.0 G_0 has already been observed for the case of H_2 on metallic Pt contacts [15]. Alternatively, ionic lead species could be taken into account, where specific transport channels of the junction are selectively suppressed. The simple interpretation of a conductance of 1.0 G_0 as a result of conductance quantization of a free electron gas in a geometrical constriction as observed in a two-dimensional electron gas (2DEG) in semiconductor heterostructures [16] and s-type metals is discussed controversially for non-s-type metals.

An alternative explanation of the peaks at 2 G_0 and 2.8 G_0 would be their interpretation as replicas of those at 1 G_0 and 1.4 G_0 with twice the value. Though geometries with parallel atomic wires were observed for gold in the case of mechanical deformation [17] no indications for the formation of similar structures were found for the case of lead so far.

6. Collaborations with other CFN Projects

Subproject B1.6 is in close collaboration with different groups and subprojects within the CFN. Especially, there is a very effective cooperation with different theory groups, which are also documented by collaborative publications (see e.g. [B1.6:1], [B1.6:2], [B1.6:9], [B1.6:11]):

- Collaboration with W. Wenzel and G. Schön (C3.6) concerning the study of quantum transport and the atomic transistor switching process based on atomic-scale bistabilities.
- Collaboration with F. Evers (B2.10) and P. Wölfle concerning electrochemical switching processes based on collective processes during contact formation and contact opening.
- Collaboration with F. Pauly and G. Schön (B1.7) on electronic transport in atomic-scale Pb contacts and the influence of the atomic-scale configuration of the contacting atom(s).

In addition, the results obtained and the preparation techniques developed within B1.6 are of increasing relevance for projects in project area A, e.g. subproject A4.4 (J. Leuthold).

References:

[1] N. Agraït, J. G. Rodrigo, and S. Vieira, Phys. Rev. B **47**, 12345 (1993).

[2] J. K. Gimzewski and R. Möller, Phys. Rev. B **36**, 1284 (1987).

[3] K. O'Neill, E. A.Osorio, and H. S. J. van der Zant, Appl. Phys. Lett. **90**, 133109 (2007).

[4] C. Schirm, H.-F. Pernau, and E. Scheer, Rev. of Sci. Instrum. **80**, 024704 (2009).

[5] C. Z. Li, A. Bogozi, W. Huang, and N. J. Tao, Nanotechnology **10**, 221 (1999).

[6] F.-Q. Xie, L. Nittler, Ch. Obermair, and Th. Schimmel, *Gate-controlled atomic quantum switch*, Phys. Rev. Lett. **93**, 128303 (2004).

[7] T. Sakamoto, N. Iguchi, and M. Aono, *Appl. Phys. Lett*. **96**, 252104(2010).

[8] E. H. Lyons, In *Modern Electroplating;* Lowenheim, F. A., Ed.; Wiley, New York, ed. 3, **1974**; pp.1-45.

[9] M. Brandbyge, K. W. Jacobsen, J. K. Norskov, *Phys. Rev. B* **55**, 2637-2650 (1977).

[10] A. I. Yanson, PhD thesis (2001).

[11] P. Makk, S. Csonka, and A. Halbritter, Phys. Rev. B **78,** 045414 (2008).

[12] J. C. Cuevas, A. Levy Yeyati, A. Martín-Rodero, G. Rubio Bollinger, C. Untiedt, and N. Agraït, Phys. Rev. Lett. **81**, 2990 (1998).

[13] C. Obermair, R. Kniese, F.-Q. Xie, and Th. Schimmel, in NATO Advanced Research Workshop on Molecular Nanowires and Other Quantum Objects, edited by A. S. Alexandrov, J. Demsar, and I. K. Yanson (Springer, Bled, SLOVENIA, 2003), pp. 233.

[14] E. Scheer, N. Agraït, J. C. Cuevas, A. L. Yeyati, B. Ludoph, A. Martín-Rodero, G. Rubio Bollinger, J. M. van Ruitenbeek, and C. Urbina, Nature **394**, 154 (1998).

[15] R. H. M. Smit, Y. Noat, C. Untiedt, N. D. Lang, M. C. van Hemert, and J. M. van Ruitenbeek, Nature **419**, 906 (2002).

[16] B. J. van Wees *et al*., Phys. Rev. Lett. **60**, 848 (1988); D. A. Wharam *et al*., J. Phys. C 21, L209 (1988).

[17] H. Ohnishi, Y. Kondo, and K. Takayanagi, Nature **395**, 780 (1998).